




Antiresorptive Agents Are More Effective in Preventing Titanium Particle-Induced Calvarial Osteolysis in Ovariectomized Mice Than Anabolic Agents in Short-Term Administration

*Guangtao Fu, *Shixun Li, †Nengtai Ouyang, ‡Junyan Wu, *Changchuan Li, *Wei Liu, *Junxiong Qiu, *Peng Peng, §Ling Qin and **Yue Ding 

**Department of Orthopedics, Sun Yat-Sen Memorial Hospital, Sun Yat-Sen University, Yuexiu District; †Cellular & Molecular Diagnostics Center, Sun Yat-Sen Memorial Hospital, Sun Yat-Sen University, Yuexiu District; ‡Department of Pharmaceuticals, Sun Yat-Sen Memorial Hospital, Sun Yat-Sen University, Yuexiu District, Guangzhou, Guangdong Province; §Musculoskeletal Research Laboratory, Department of Orthopaedics & Traumatology, The Chinese University of Hong Kong, Hong Kong SAR; and **Guangdong Provincial Key Laboratory of Malignant Tumor Epigenetics and Gene Regulation, Sun Yat-Sen Memorial Hospital, Sun Yat-Sen University, Yuexiu District, Guangzhou, Guangdong Province, People's Republic of China*

Abstract: Aseptic loosening due to wear particle-induced osteolysis is the main cause of arthroplasty failure and the influence of postmenopausal osteoporosis and anti-osteoporosis treatment on Titanium (Ti) particle-induced osteolysis remains unclear. 66 C57BL/6J female mice were used in this study. Ovariectomy (OVX) was performed to induce osteopenia mice and confirmed by micro-CT. The Ti particle-induced mouse calvaria osteolysis model was established subsequently and both OVX and Sham-OVX mice were divided into four groups, respectively: Ti (-) group, Ti group, Ti + zoledronic acid (ZOL) group (50ug/kg, local administration, single dose) and Ti + teriparatide (TPTD) group (40ug/kg/d, subcutaneous injection*14d). Mice calvarias were collected for micro-CT and histomorphometric analysis 2 weeks after particle induction. 8 weeks after bilateral OVX, significantly reduced BMD and microstructure parameters in both proximal tibia and calvaria were observed in OVX mice when comparing with Sham-OVX mice. OVX mice in Ti group had not only markedly decreased BMD and

BV/TV, but also significantly increased total porosity, eroded surface area and osteoclast numbers when comparing with Sham-OVX mice. Shown by Two-way ANOVA analysis, the interaction terms between OVX and Ti implantation on micro-CT and histomorphometry parameters didn't reach significant difference. As illustrated by micro-CT and histological analysis, ZOL treatment markedly inhibited Ti particle-induced osteolysis in OVX mice and Sham-OVX mice, and there were significant differences when comparing to both Ti and Ti+TPTD group. The combination of osteoporosis and Ti particle implantation result in aggravated bone resorption, accompanied with increased osteoclasts and excessive inflammation response. ZOL was more effective in preventing Ti particle-induced osteolysis in both OVX mice and Sham-OVX mice than TPTD in short-term administration. ZOL exert the protective effects on Ti particle-induced bone loss via the suppression of osteoclasts. **Key Words:** Ovariectomy—Wear particle—Osteolysis—Anabolics—Antiresorptives.

doi: 10.1111/aor.13271

Received January 2018; revised March 2018; accepted April 2018.

Guangtao Fu and Shixun Li contributed equally to this work. Address correspondence and reprint requests to Yue Ding, Department of Orthopedics, Sun Yat-sen Memorial Hospital, Sun Yat-sen University, 107 Yanjiangxi Road, Yuexiu District, Guangzhou, Guangdong Province, People's Republic of China. E-mail: dingyue36@126.com or Ling Qin, Musculoskeletal Research Laboratory, Department of Orthopaedics & Taumatology, the Chinese University of Hong Kong, Hong Kong SAR, Guangzhou, Guangdong Province, People's Republic of China. E-mail: b664730@mailserv.cuhk.edu.hk

Postmenopausal osteoporosis is one of the most common primary bone metabolic disorders in elderly females, characterized by significant bone loss, deterioration of bone microarchitecture, and increased risk of fragility fractures (1). Commonly used antio-osteoporosis drugs can be classified as antiresorptive and anabolic agents, while the representative drugs are zoledronate (ZOL) and teriparatide (TPTD), respectively. More than half of the females over 50 years suffer an osteoporotic fracture during their

lifetime and subsequently require huge number of orthopedic procedures, including total hip arthroplasty (THA) (2). It is reported that more than half of the patients undergoing THA are combined with osteoporosis (3). Being the most effective method for the treatment of end-stage hip disease, the long-term functional outcome of THA and the service life of prostheses are greatly limited by wear particle-induced periprosthetic osteolysis and subsequent aseptic loosening, with the overall arthroplasty failure rate of 16% 20 years postoperation (4,5). To date, the only established treatment for aseptic loosening is total hip revision, which is associated with not only significant medical cost but also technical difficulty and poor functional outcome. Fully understanding of the pathophysiology and new medicine treatment strategy for the prevention and treatment of aseptic loosening are strongly needed. Allowing the quantification of particle-induced osteoclastogenesis and osteolysis, titanium (Ti) particle-induced calvarial osteolysis mice model is the most common used animal model in estimating the pathophysiology of wear particle-induced periprosthetic osteolysis and aseptic loosening (6).

Highly significant relationships were found between postoperative periprosthetic bone loss and preoperative bone mineral density (BMD) measured at spine, total hip, and total distal radius (7,8). Recently, it was reported that female patients with low preoperative systemic BMD showed greater bone loss in femoral calcar after cementless THA (9). Low BMD was also reported to be associated with delayed osseointegration, accelerated implant migration, and worse initial stability (10,11). Based on the results of former mentioned studies that preoperative BMD measured at spine, hip, and forearm were major factors influencing periprosthetic bone loss and implant micromotion, we proposed that osteoporosis is the risk factor of aseptic loosening. Previous studies demonstrated that antiosteoporosis treatment significantly inhibits wear particle-induced osteoclast formation in vitro (12). Epidemiology data also revealed that the use of antiosteoporosis drugs markedly reduces the overall risk of revision after THA (13). However, the exact influence and mechanism of osteoporosis, antiresorptive, and anabolic agents on particle-induced osteolysis in vivo still remains unclear. We hypothesized that the ovariectomy (OVX)-induced osteopenia accelerates Ti particle-induced calvarial osteolysis in mice, while antiresorptive and anabolic agents have protective effect on it.

MATERIALS AND METHODS

Animals

About 66 C57/BL6J female mice, aged 7–8 weeks, were purchased from the Laboratory Animal Research Center of Sun Yat-Sen University. All experiments were approved by the Institutional Animal Care and Use Committee of Sun Yat-Sen University (approval No. IACUC-DB-16-0307), and the Guidelines for Care and Use of Laboratory Animals were strictly followed. Each of the mice weighed 20–25 g at the beginning of the study. All mice had free access to food and water.

Bilateral OVX

Six mice were randomly selected for micro-CT scanning at proximal tibia as the baseline at the age of 12 weeks and the rest of the mice were randomly and equally divided into OVX group and Sham-OVX group. Mice in both groups underwent surgeries under general anesthesia with pentobarbital (1%, 50 mg/kg, intraperitoneal injection) at the age of 12 weeks. As previous described (14), the fallopian tube and the fat pad containing the ovary were removed on both sides and were stained by HE staining to confirm the success of OVX surgery in OVX group. In Sham-OVX group, the ovaries were surgically identified but not removed. The skin incision was closed with absorbable sutures. About 8 weeks after operation, 6 mice were randomly selected from the OVX group and Sham-OVX group for micro-CT scanning at the proximal tibia.

Micro-CT scanning at proximal tibia

All the mice selected for micro-CT scanning were sacrificed and bilateral tibias were fixed in 10% formaldehyde after removal of all soft tissues. The fixed tibias were analyzed using micro-CT (SkyScan 1176; SkyScan, Kontich, Belgium) at an isometric resolution of 18 μm . Images were acquired at 45 kV and 500 μA through a 0.2 mm-thick aluminum filter with an exposure time of 240 ms. The manufacturer's software (NRecon, SkyScan) was used to reconstruct three-dimensional (3D) images based on the radiographs. BMD (g/cm^3) and morphometric parameters, including bone volume fraction (BV/TV, %), trabecular thickness (Tb. Th, μm), and trabecular separation (Tb. Sp, μm) were measured from 1 to 2 mm distal to the growth plate of proximal tibias in the long axis. About 60 continuous sections were analyzed with CTAn software (SkyScan). Description and nomenclatures were strictly according to the

guidelines for the assessment of bone microstructure using micro-CT analysis (15).

Preparation of Ti particles

Commercial pure Ti particles were purchased from Alfa Aesar (Ward Hill, MA, USA). These particles were diluted with pure water and filtered by Millipore filter membranes (pore diameter: 1.0 μm , Billerica, MA, USA). Ti particles (diameter: $0.82 \pm 0.12 \mu\text{m}$) were obtained after filtration. All Ti particles were washed with 75% ethanol and dried in a biological drying oven. The dried Ti particles were sterilized with ethylene oxide. The absence of endotoxin in Ti particles was confirmed by commercial limulus assay kit (QCI-1000; Bio Whittaker, Walkersville, MD, USA). The Ti particles were stored in sterile phosphate buffered saline (PBS) at 4°C after being washed with sterile PBS for three times.

Ti particle-induced mouse calvaria osteolysis model

The Ti particle-induced mouse calvaria osteolysis model was established in the rest of the OVX ($n=24$) and Sham-OVX mice ($n=24$) at the age of 20 weeks. Mice in both groups were subdivided into four groups: Ti (-) group, Ti group, Ti+ZOL group, and Ti+TPTD group, respectively. Animals underwent surgeries under anesthesia with pentobarbital (1%, 50 mg/kg, intraperitoneal injection). As previously described (16), the hair overlying the skull was carefully shaved and the surgical field was sterilized with 75% ethanol for three times. After being exposed by making a 1 cm midline sagittal incision, the periosteum of the calvaria was scraped using a surgical scalpel in all groups. In Ti, Ti+ZOL, and Ti+TPTD group, 50 μL PBS containing 0.3 mg Ti particles was spread onto the center of the calvaria. In Ti+ZOL group, single dose 25 μL ZOL (50 $\mu\text{g}/\text{kg}$, Novartis Pharma Stein AG, Stein, Switzerland) was injected into the space between the calvaria and the skin, which was modified from von Knoch's study (17). Ti+TPTD group received consecutive TPTD (rh [1–34] PTH, 40 $\mu\text{g}/\text{kg}/\text{day}$, as previous recommended (18), subcutaneous injection, Lilly, France) for 14 days. A similar volume (25 μL) of PBS was injected locally into calvaria of Ti group and Ti+TPTD group as well. Mice from Ti (-) group received 75 μL PBS without particles. The skin incision was closed with absorbable sutures. No mice died and no wound complications were observed during the experiments. Mice were sacrificed in a CO_2 chamber 14 days after surgery, and the calvarias were harvested for micro-CT scanning and histological analysis.

Micro-CT imaging of mice calvaria

The harvested calvarias were fixed in 10% formaldehyde for 2 days after the removal of all soft tissues. Then the fixed calvarias were analyzed by micro-CT and associated analysis software as previously described. The scanning protocol was set at an isometric resolution of 18 μm , and radiographs were acquired at 45 kV and 500 μA through a 0.2 mm-thick aluminum filter with an exposure time of 240 ms. The 3D image reconstructions were obtained using the manufacturer's software. As previously described (19), a square-shaped region of interest (ROI) of 3 mm \times 1 mm, with the midline suture in its center, was placed in the 2D reconstructed cross-section slices in the middle of the sagittal suture on coronal plane. Then, ROIs were combined in order to form a volume of interest (VOI) of 3 mm \times 1 mm \times 3 mm for further quantitative analysis. BV/TV, BMD, and total porosity of each sample were obtained with CTAn software.

Histological and immunohistochemical analysis

All the calvarias were decalcified in 10% ethylene diamine tetraacetic acid (EDTA) for 21 days and then embedded in paraffin after micro-CT scanning. Cross-sections (4 μm) were cut and stained with hematoxylin and eosin (H&E), commercial tartrate resistant acid phosphatase (TRAP) staining kit (Jiancheng Bioengineering Institute, Nanjing, China) and alkaline phosphatase (ALP) staining kit (Jiancheng Bioengineering). Histological sections were analyzed using a standard high-quality light microscope (DM2000, Leica, Wetzlar, Germany) at a magnification of 10 \times with the midline suture in its center. Histomorphometric analysis was performed on the most central section and four adjacent sections using image analysis software (Image Pro-Plus 6.0, Media Cybernetics, Bethesda, MD, USA). The region of interest (ROI) was defined as previously recommended (20). The eroded bone area (mm^2) was determined by tracing the area of soft tissue between the parietal bones, including resorption pits on the superior surface of the calvaria. The number of osteoclasts and osteoblasts were determined within the ROI. As previous described (21), the presence of dark-purple-stained granules in the TRAP staining section, which located on the bone perimeter within a resorption lacuna, was defined as osteoclasts. The presence of dark gray-stained granules within the cytoplasm in the ALP staining section was defined as osteoblasts. For histological detection of RANKL, TNF- α , IL-1 β , and OPG (Abcam, Shanghai, China), sections were dewaxed using xylene, gradient ethanol, and PBS sequentially, followed by endogenous

peroxidase blocking with 3% hydrogen peroxide for 10 min. Antigen retrieval was performed using citric acid with water bath at 60°C for 15 min, and then cooled to room temperature. After incubated with goat anti-mouse IgG for 10 min at 37°C, the sections were incubated with primary antibodies for RANKL, TNF- α , IL-1 β , and OPG at 4°C overnight. After washing, sections were incubated with appropriate secondary antibodies at 37°C for 60 min. Coloration of sections were performed with 3,3-diaminobenzidine (DAB), keeping at room temperature without light for 2 min. Rinsed sections were counterstained with hematoxylin. The nomenclature and methods used were according to the recommendation of the Nomenclature Committee of the American Society for Bone and Mineral Research (22).

Statistical analysis

All quantitative data are presented as mean \pm standard deviation (SD). All values were first assessed using a Kolmogorov–Smirnov test to ensure normality and Gaussian distribution. Two-sided Student's *t*-test was used for the comparison between Sham OVX-Ti (-) and OVX-Ti (-) group, and the comparison between Sham OVX-Ti and OVX-Ti group. One-way analysis of variance (ANOVA) was used for the comparison among Sham OVX-Ti (-), Sham OVX-Ti, Sham OVX-Ti+ZOL, and Sham OVX-Ti+TPTD group, and another ANOVA was used for the comparison among OVX-Ti (-), OVX-Ti, OVX-Ti+ZOL, and OVX-Ti+TPTD group. Post hoc comparison between groups used the Fisher's protected least significant difference. Two-way ANOVA containing Sham OVX-Ti (-), Sham OVX-Ti, OVX-Ti (-), and OVX-Ti was performed to evaluate the effects due to OVX, effects due to Ti implantation and the interaction terms between OVX and Ti particle implantation on micro CT and histological parameters. A *P* value of <0.05 was considered to be significant. SPSS 20.0 software (SPSS, Chicago, IL, USA) was used to carry out the statistical analysis.

RESULTS

Micro-CT scanning of proximal tibia

About 8 weeks after bilateral OVX, deterioration of the trabecular architecture in proximal tibia was readily observed in gross observation by 3D images (Fig. 1A). OVX mice had significantly reduced BMD, BV/TV, Tb.Th, and markedly increased Tb.Sp when compared to the mice at 12 weeks (Fig. 1B–D). Similar results were obtained when

comparing with the mice at 20 weeks (Fig. 1B–D). Besides, we found no significant difference of the former mentioned parameters between the mice at 12 and 20 weeks.

Micro-CT scanning of Ti particle-induced calvaria osteolysis

The 3D reconstruction images revealed that Ti particles induced profound changes in calvarial bone microarchitecture in both OVX and Sham-OVX mice (Fig. 2). Quantitative analysis showed that OVX mice had significantly decreased BMD and BV/TV when comparing with Sham-OVX mice in the Ti (-) group (Fig. 3A,B). More severe bone resorption was observed in the calvaria of OVX mice with stimulation of Ti particles when comparing with Sham-OVX mice, with significantly decreased BMD and BV/TV, as well as increased total porosity (Fig. 3). Two-way ANOVA revealed that the interaction term between OVX and Ti particle implantation on BMD, BV/TV, and total porosity did not reach significant levels. In addition, Ti particle-induced bone resorption was markedly inhibited when treated with ZOL in both OVX mice and Sham-OVX mice, with significant improvement of BMD, BV/TV, and total porosity (Fig. 4). However, there was only a significantly increased BMD in OVX mice when comparing with Ti group after 2 weeks TPTD administration (Fig. 4D). In addition, there were also significant differences between the Ti+ZOL and Ti+TPTD group of BMD, BV/TV, and total porosity in OVX mice, and of BV/TV and total porosity in Sham-OVX mice.

Bone histomorphometry

As illustrated by H&E and TRAP staining, Ti particles induced erosion of the calvarial bone with intense inflammatory infiltration and multiple TRAP positive cells accumulating along the eroded bone surface when compared with Ti (-) group in both OVX and Sham-OVX mice (Fig. 5A,B). More severe bone erosion and more TRAP positive cells were also observed in OVX mice than in Sham-OVX mice when stimulated with Ti particles (Fig. 6A,B). Two-way ANOVA revealed that the interaction term between OVX and Ti particle implantation on bone erosion area and TRAP positive cell numbers did not reach a significant level. Consistent with the micro-CT quantification, the tissue response to Ti particles appeared limited in both OVX and Sham-OVX mice when treated with ZOL, with significant reduction of eroded surface area and TRAP positive cell number (Fig. 7). Histomorphometric results also revealed that there was significant decrease in eroded surface area in Ti+TPTD group (Fig. 7A,D).

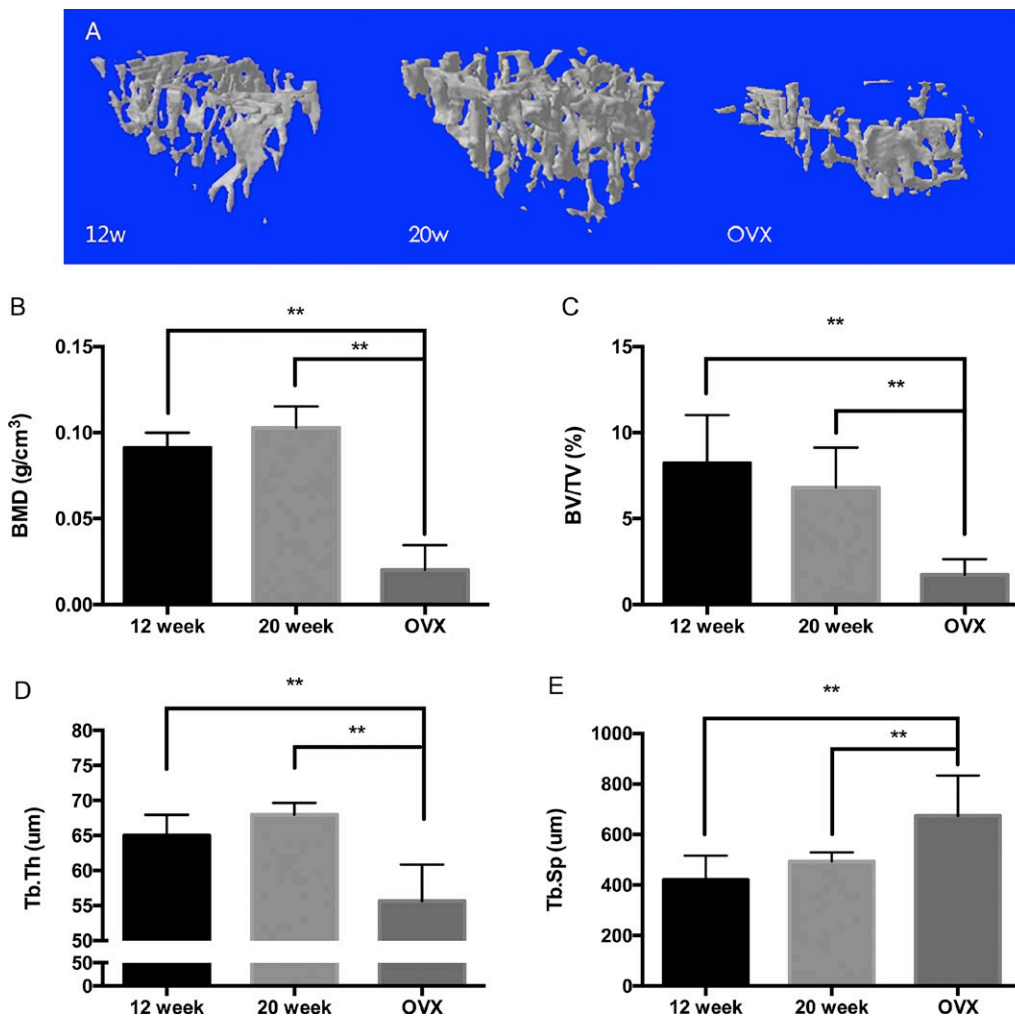


FIG. 1. Establishment of the OVX-induced osteopenia mice model. (A) Representative micro-CT 3D reconstructed images of proximal tibia obtained from each group ($N=6$ per group). (B–D) Comparison of BMD, BV/TV, Tb.Th, and Tb.Sp. ($N=6$ per group); * indicated $P < 0.05$ and ** indicated $P < 0.01$, determined by one-way ANOVA and least significant difference (LSD) test. Error bars in the graph represent standard error. [Color figure can be viewed at wileyonlinelibrary.com]

In addition, there were also significant differences between the Ti+ZOL and Ti+ TPTD group of TRAP positive cell numbers in OVX mice, and of eroded bone area and TRAP positive cell numbers in Sham-OVX mice. We found that there were only a small amount of osteoblasts within the ROI in all mice (Fig. 5C), with no significant difference of the number of ALP positive cells between all the groups (Fig. 7C,F).

Immunochemical analysis of TNF- α , RANKL, IL-1 β , and OPG

Localizing primarily in the inflammatory cells around the eroded bone surface, positive staining of TNF- α , RANKL, and IL-1 β were observed in Ti group and seemed more obvious in OVX mice

(Fig. 8). After ZOL treatment, few positive staining reactions for these inflammatory cytokines were observed in either OVX or Sham-OVX mice, while there was a slightly increased expression of OPG (Fig. 8). There were still positive staining of OPG, TNF- α , RANKL, and IL-1 β in both OVX and Sham-OVX mice after TPTD treatment.

DISCUSSION

A 12-week-old mouse is sexually mature and capable of responding appropriately to OVX (23). In the present study, severe deterioration of the trabecular architecture in proximal tibia and significant decrease of BMD and BV/TV in calvaria were observed in OVX mice without Ti particle

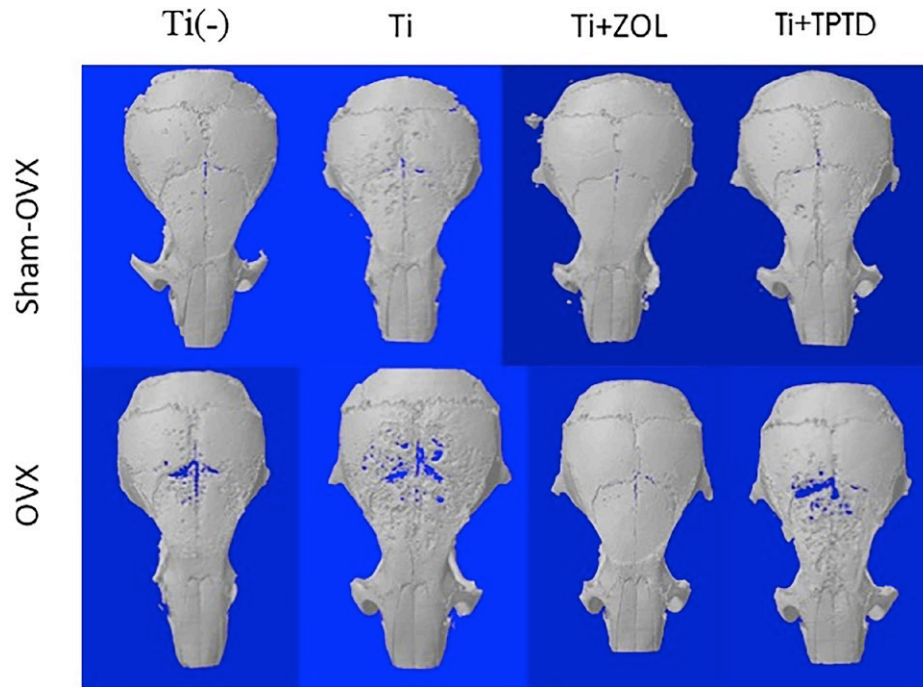


FIG. 2. Representative micro-CT 3D reconstructed images obtained from each groups ($N=6$ per group). [Color figure can be viewed at wileyonlinelibrary.com]

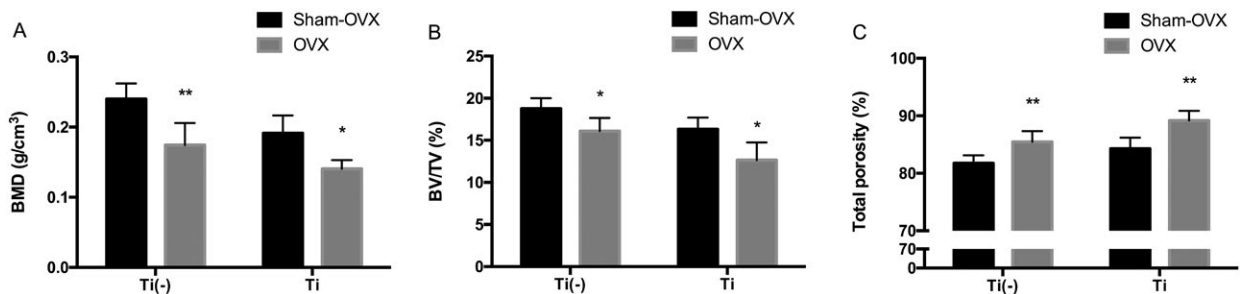


FIG. 3. Evaluation of the influence of OVX on Ti particle-induced calvaria osteolysis via micro CT quantitative analysis. BMD (A), BV/TV (B), and the total porosity (C) of each sample within the ROI were measured ($N=6$ per group). Two-sided Student's *t*-test was used for the comparison between Sham OVX-Ti (-) and OVX-Ti (-) group, and the comparison between Sham OVX-Ti and OVX-Ti group. Two-way ANOVA containing Sham OVX-Ti (-), Sham OVX-Ti, OVX-Ti (-), and OVX-Ti was performed to evaluate the effects due to OVX, effects due to Ti implantation and the interaction terms between OVX and Ti particle implantation. * indicated $P < 0.05$ and ** indicated $P < 0.01$. Error bars in the graph represent standard error.

stimulation, which demonstrated that the OVX-induced osteopenia mice model was successfully established, with both tibia and calvaria affected. Afterward, we compared the Ti particle-induced calvaria osteolysis of C57/BL6J female OVX mice with age-matched Sham-OVX mice. As expected, the presence of Ti particles induced profound changes in calvarial bone of both OVX and Sham-OVX mice, which was consistent with previous studies (6). Previous research showed that the chronic inflammatory response to wear particles involving macrophages, osteoclasts and osteoblasts plays

a pivotal role in the initiation and development of aseptic loosening (24,25). Macrophages produce more proinflammatory cytokines (TNF- α , IL-6, IL-1 β , and RANKL) after Ti particle stimulation. The upgraded proinflammatory cytokines secretion induces differentiation and activation of osteoclasts and subsequent osteolysis, which is regulated by the size, shape, and density of the wear particles (26,27). Moreover, a large number of macrophages with massive expression of Toll-like receptors (TLRs) had been found in the synovial membrane samples from aseptic loosening patients, indicating that wear

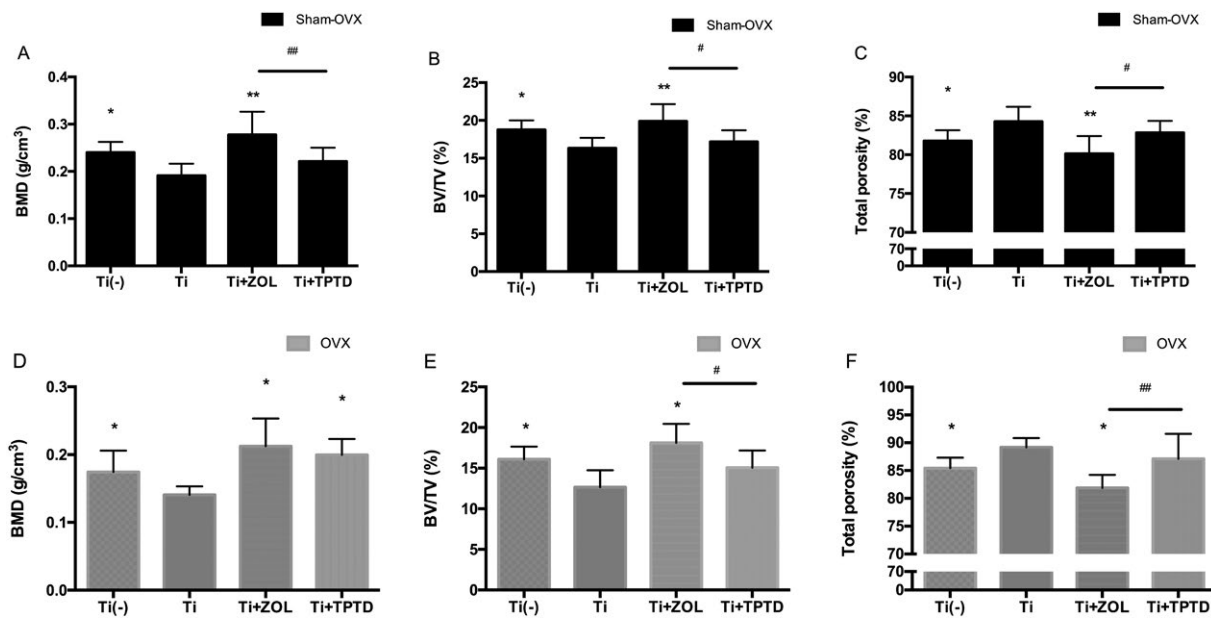


FIG. 4. Evaluation of the effect of ZOL and TPTD on Ti particle-induced calvaria osteolysis via micro-CT quantitative analysis. $N=6$ per group. One-way ANOVA was used for the comparison among Sham OVX-Ti (-), Sham OVX-Ti, Sham OVX-Ti+ZOL, and Sham OVX-Ti+TPTD group, and there were another ANOVA for the comparison among OVX-Ti (-), OVX-Ti, OVX-Ti+ZOL, and OVX-Ti+TPTD group. Post hoc comparison between groups used the Fisher's protected least significant difference. * indicated $P < 0.05$ and ** indicated $P < 0.01$, when comparing to Ti group. # indicated $P < 0.05$ and ## indicated $P < 0.01$ in the comparison between Ti+ZOL and Ti+TPTD group. Error bars in the graph represent standard error.

particles might activate the macrophages through pattern recognition receptors (PRRs) (28). However, the exact mechanism of particle-induced osteolysis is not entirely clear and further investigation is needed.

Illustrated by micro-CT and histology, Ti particle-induced osteolysis in the calvarial bone was much more obvious in OVX mice when comparing with Sham-OVX mice. However, the results reported by Nich's group are not entirely consistent with ours (29–31). Those studies performed the surgery for building the particle-induced mouse calvaria osteolysis model just 1 week after bilateral OVX, without using micro-CT to confirm the establishment of osteopenic mouse model by comparing the BMD and microstructure parameters of OVX mice to Sham-OVX mice. It is well known that BMD measurement is essential for the clinical diagnosis of osteoporosis and results of most studies indicated that it takes 7–9 weeks to build the osteopenic mouse model after OVX (32,33), which is consistent with our study. Thus, we consider that Nich's studies actually built the animal model of estrogen deficiency, rather than osteopenia, which could not demonstrate the exact influence of osteopenia on particle-induced osteolysis in mice. It was reported that estrogen has both pro- and anti-inflammatory properties, which

is dependent on situation (i.e., doses and estrogen receptor distribution) (34,35). That may be another reasonable explanation for the inconsistent results between ours and Nich's study. However, the present study could not come to the conclusion that osteopenia played a role on Ti particle-induced osteolysis, as the interaction term on micro-CT and histomorphometry measurement did not reach significant difference. Further animal and clinical studies are underway to further investigate this issue.

In the present study, OVX mice in the Ti group had more osteoclasts within the ROI than the Sham-OVX mice, with significantly aggravated bone resorption. In view of the critical role that osteoclasts play in the initiation of both wear particle-induced osteolysis and osteoporosis-related bone loss (1,25), we considered that the aggravation of osteolysis on calvarial bone in OVX mice is associated with increased osteoclastogenesis after the combination of two inflammation-related bone resorptive situations. Previous study also had similar results that postmenopausal osteoporosis enhanced inflammation-induced bone remodeling with increased osteoclast activity (36). RANKL is one of the essential cytokines required for osteoclast formation, which promotes the differentiation of osteoclast precursors into fully mature multinucleated osteoclasts and

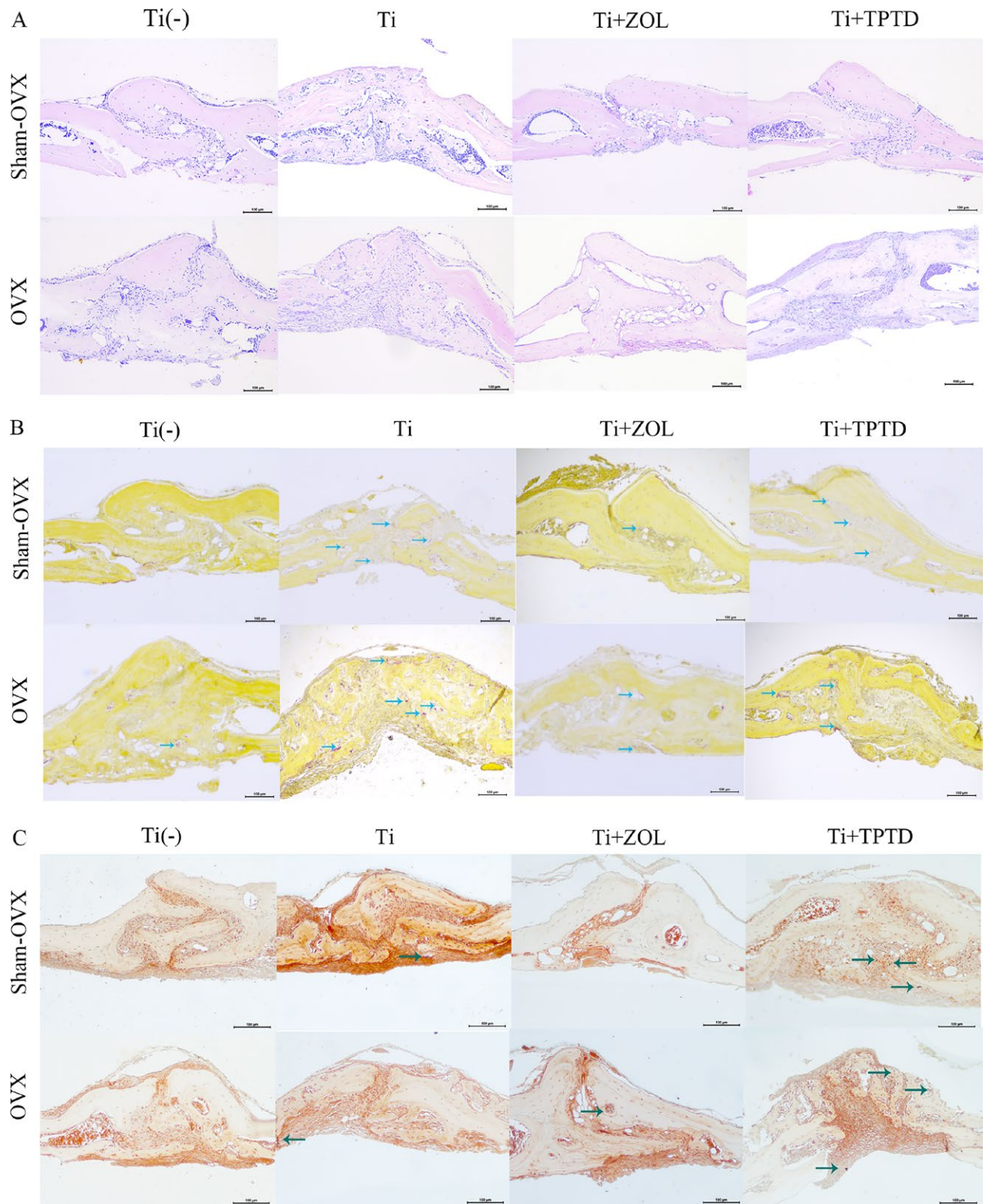


FIG. 5. Representative histological slices of HE staining (A), TRAP staining (B), and ALP staining (C) obtained from each group at a magnification of 10 \times . ($N=6$ per group). The blue arrows indicate osteoclasts (B) and osteoblasts (C). Scale bar: 100 μm . [Color figure can be viewed at wileyonlinelibrary.com]

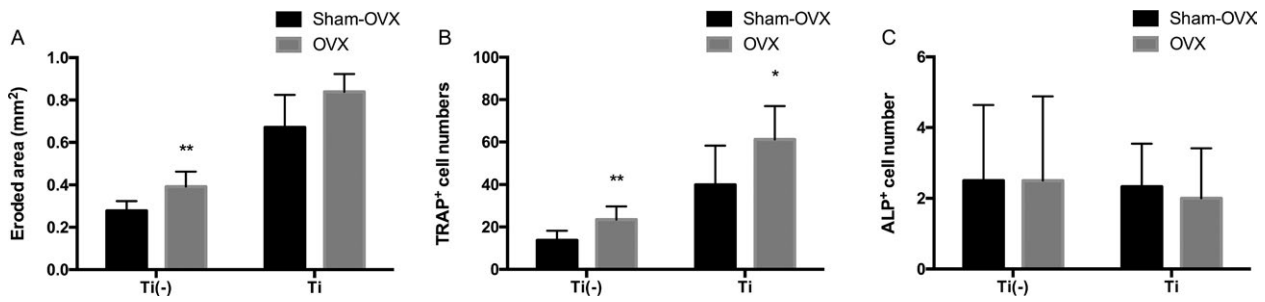


FIG. 6. Evaluation of the effect of OVX on Ti particle-induced calvaria osteolysis via histomorphometric analysis. The eroded surface area (A), the number of TRAP positive multinucleated osteoclasts (B), and the number of ALP positive osteoblasts (C) within the ROI were measured (N=6 per group). Two-sided Student's *t*-test was used for the comparison between Sham OVX-Ti (-) and OVX-Ti (-) group, and the comparison between Sham OVX-Ti and OVX-Ti group. Two-way ANOVA containing Sham OVX-Ti (-), Sham OVX-Ti, OVX-Ti (-), and OVX-Ti was performed to evaluate the effects due to OVX, effects due to Ti implantation and the interaction terms between OVX and Ti particle implantation. * indicated *P* < 0.05 and ** indicated *P* < 0.01. Error bars in the graph represent standard error.

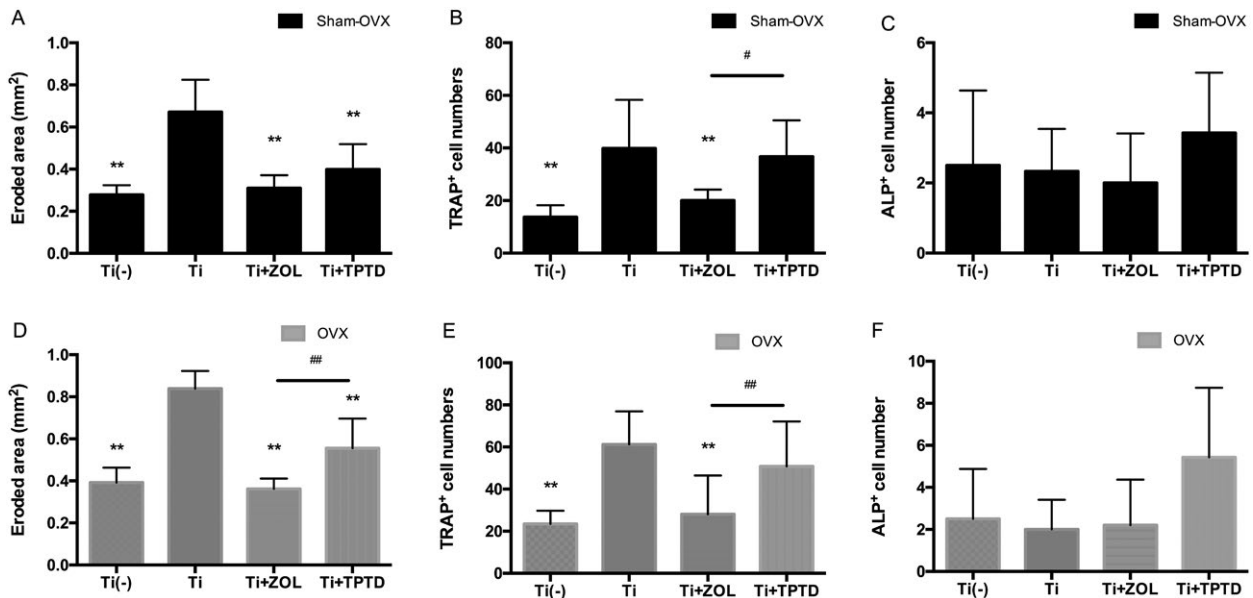


FIG. 7. Evaluation of the effect of ZOL and TPTD on Ti particle-induced calvaria osteolysis via histomorphometric analysis. N=6 per group. One-way ANOVA was used for the comparison among Sham OVX-Ti (-), Sham OVX-Ti, Sham OVX-Ti+ZOL, and Sham OVX-Ti+TPTD group, and another ANOVA was used for the comparison among OVX-Ti (-), OVX-Ti, OVX-Ti+ZOL, and OVX-Ti+TPTD group. Post hoc comparison between groups used the Fisher's protected least significant difference. * indicated *P* < 0.05 and ** indicated *P* < 0.01, when comparing to Ti group. # indicated *P* < 0.05 and ## indicated *P* < 0.01 in the comparison between Ti+ZOL and Ti+TPTD group. Error bars in the graph represent standard error.

stimulates the capacity of mature osteoclasts to resorb bone (37). The unbalance between RANKL and OPG is indicated as the pivotal mechanism of both estrogen deficiency bone loss and particle-induced osteolysis through controlling the activation state of osteoclasts (24,37,38). It was recently reported that inhibition of RANKL-induced osteoclastogenesis prevents both OVX-induced osteoporosis and wear particle-induced osteolysis (39). Additional inflammatory cytokines are reported to be responsible

for the up-regulation of osteoclasts formation, and those most involved in bone loss appear to be TNF- α and IL-1 β . TNF- α is considered to act by increasing RANKL expression in macrophages and stromal cells, which is up regulated by IL-1 β (40). Further studies also supported the critical role of pro-inflammation factors in both particle-induced osteolysis and postmenopausal osteoporosis (24,41). Illustrated by immunohistochemical analysis, positive staining of TNF- α , RANKL, and IL-1 β were observed in the

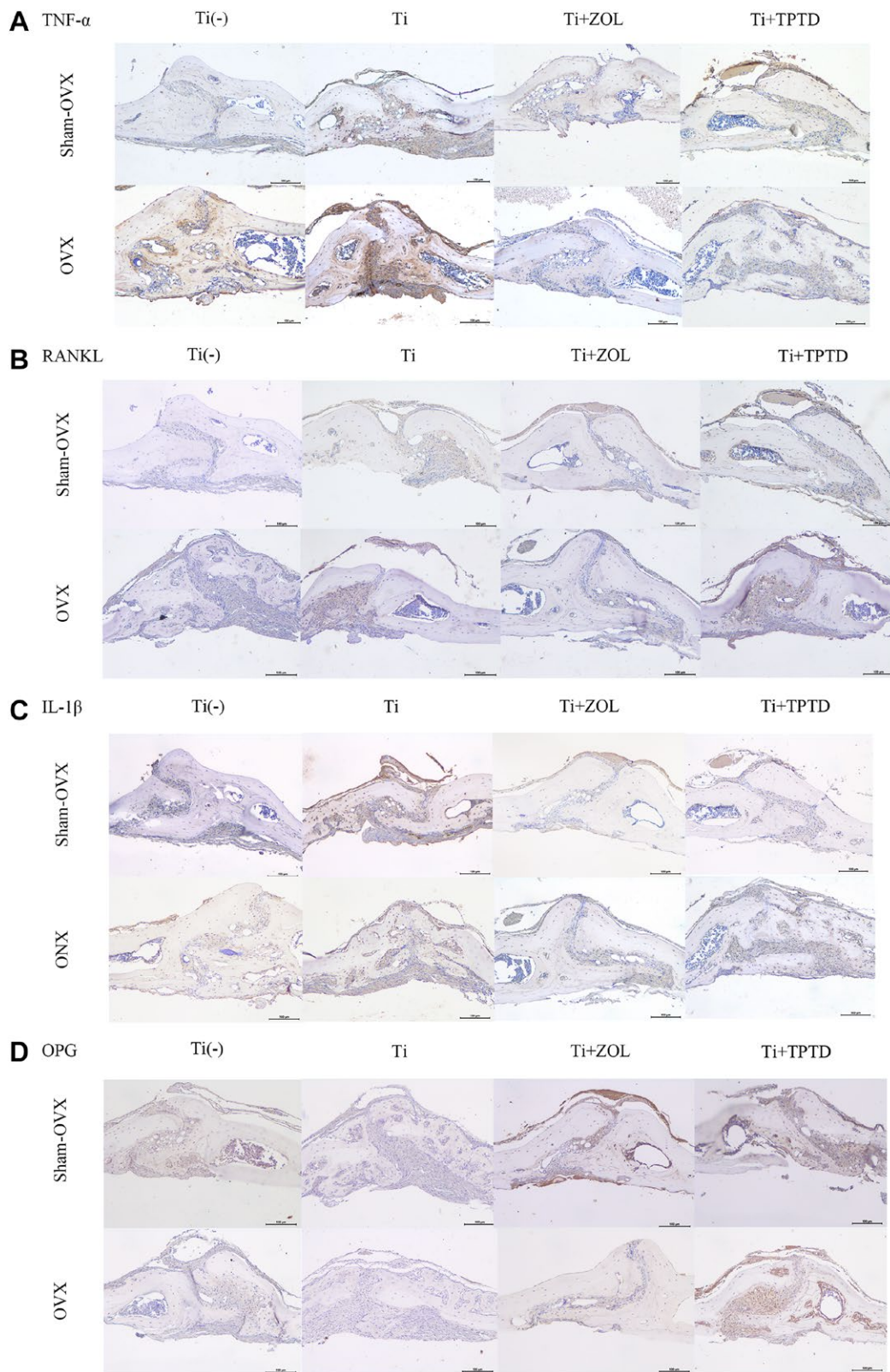


FIG. 8. Immunohistochemical staining for TNF- α (A), RANKL (B), IL-1 β (C), and OPG (D) in mouse calvaria ($N=6$ per group). Scale bar: 100 μ m. [Color figure can be viewed at wileyonlinelibrary.com]

Ti group, which seems more obvious in OVX mice. According to the present study, we considered that the combination of two bone resorptive situations might result in an excessive inflammation response with local upgraded pro-inflammatory cytokines. Quantitative analysis is needed to further investigation of the involvement of inflammation cytokines.

ZOL is a widely used third-generation bisphosphonate, which has been proven to be a useful antiresorptive agent for postmenopausal women via the suppression of the osteoclasts activity (42). As illustrated by micro-CT and histology, we found that ZOL treatment markedly inhibited bone resorption induced by Ti particles in both OVX mice and Sham-OVX mice. Epidemiology data showed that the use of bisphosphonates markedly reduces the risk of revision after THA (13), which is consistent with the findings of the present study. Bisphosphonate inhibits bone resorption mostly by reducing the activity of osteoclasts through inhibiting farnesyl pyrophosphate synthase activity and by reducing the population of osteoclast precursor cells (43). However, the exact mechanism of the protective effect of ZOL on particle-induced calvaria osteolysis in OVX mice has not yet been entirely clarified. The current study found that ZOL significantly reduced the number of TRAP positive cells in both OVX mice and Sham-OVX mice when comparing with the Ti group, which was consistent with previous study (44). Thus, we proposed that the ZOL exerts the protective effects on Ti particle-induced bone loss via the suppression of osteoclasts. Illustrated by immunochemical analysis, there was increase expression of OPG and marked inhibition of the expression of RANKL, TNF- α , and IL-1 β after ZOL treatment. It was reported that ZOL inhibited the recruitment and differentiation of osteoclasts by reducing transmembrane RANKL expression and increasing OPG secretion in osteoblast-like cells (45). The secretion of TNF- α of macrophages (RAW264.7) stimulated by wear particles could be reduced by alendronate, another bisphosphonate (12). Taken together, we considered that the ZOL exerts an anti-inflammation effect in addition to its direct effects on mature osteoclasts, which represents another potential cause of the protective effects on Ti particle-induced bone loss.

TPTD is an anabolic drug that works primarily through remodeling, which firstly requires activation of osteoclasts to resorb bone, followed by replacing more bone than removed through the stimulation of osteoblast activity to achieve a net increase in bone mass (46). It was reported that daily injection with TPTD (40 mg/kg/day) for 7 weeks significantly enhanced femoral bone strength, which was associated

with improvement of femoral BMD, bone markers, and bone structure (18). In addition, several clinical case reports found that patients diagnosed with prosthetic aseptic loosening experience clinical improvement with disappearance of radiographic signs of loosening after 6–8 months TPTD treatment, indicating that TPTD may be a potential new alternative treatment for the prevention of particle-induced periprosthetic osteolysis and sequential aseptic loosening (47,48). However, results of the present study indicated that 2 weeks of TPTD treatment could not inhibit the Ti particle-induced bone resorption in OVX and Sham-OVX mice as effective as ZOL, which was contradictory with our hypothesis. As TPTD treatment aimed at osteoporosis prevention or fracture healing promotion in mice model mostly lasted for 4–6 weeks (49,50), we hypothesized that the unsatisfactory protective effect on Ti particle-induced calvaria osteolysis of TPTD in the present study may due to the insufficient duration of treatment. Further animal studies are underway to test this hypothesis with prolonged duration (i.e., 4–6 weeks) of TPTD administration.

This study was subjected to some limitations. Firstly, the osteolysis process lasted for only 2 weeks, representing an acute inflammatory process rather than a chronic one. Thus, the clinical relevance of the murine calvaria model should be considered with caution. Secondly, it was reported that ultra-high molecular weight polyethylene (UHMWPE) particles are the main cause of periprosthetic osteolysis (12). However, it was found that Ti particles could also effectively activate osteoclast formation and function to induce osteolysis *in vivo*, remaining one of the crucial causes of aseptic loosening (16,51). Thus, we believe that both Ti particles and UHMWPE particle-induced models are suitable to investigate the effects of osteoporosis and antiosteoporosis treatment on bone resorption. Lastly, drugs with same administration method are more comparable. In the present study, ZOL was given in a single dose and the TPTD was given consecutively, which was based on the clinical practice. The method of TPTD administration is consistent with other *in vivo* studies using mouse models (18,49). Local administration is also common in studies evaluating the inflammatory effect of bisphosphonate drugs and prevention effect of ZOL on particle-induced osteolysis (17,52). There are also many studies comparing the effect of single dose ZOL and consecutive administration of TPTD on bone structure, osteoporotic fracture healing and the prevention of disuse osteopenia in small animal models (53–55). Taken together, we supposed that the way we compared those two drugs is acceptable

and interpretable, which can provide preliminary research foundation for clinical considerations.

CONCLUSION

The combination of osteoporosis and Ti particle implantation resulted in aggravated bone resorption, accompanied with increased osteoclasts and excessive inflammation response. ZOL was more effective in preventing Ti particle-induced osteolysis in both OVX mice and Sham-OVX mice than TPTD in short-term administration. ZOL exerts protective effects on Ti particle-induced bone loss via the suppression of osteoclasts.

Acknowledgments: This work was supported by the National Natural Science Foundation of China (81672186), the provincial science and technology project of science and technology department of Guangdong Province, China (2014B020212004, 2014A020212134), and the Yat-sen clinical research training project of Sun Yat-sen Memorial Hospital, Sun Yat-sen University (2014).

Author Contributions: Study design and approved the final version: Yue Ding. Drafting and revising the manuscript content: Guangtao Fu. Study conduct: Guangtao Fu, Shixun Li and Nengtai Ouyang. Counseling of the administration of antio-osteoporosis drugs on mice: Junyan Wu. Data collection: Changchuan Li, Junxiong Qiu, Data analysis: Wei Liu, Peng Peng. Coordination and assistance in article preparation: Ling Qin. Yue Ding takes responsibility for the integrity of the data analysis.

Conflict of Interest: Guangtao Fu, Shixun Li, Nengtai Ouyang, Junyan Wu, Changchuan Li, Wei Liu, Junxiong Qiu, Peng Peng, Ling Qin, and Yue Ding declare that they have no financial or personal relationships with other people or organizations that can inappropriately influence our work. There is no professional or other personal interest of any nature or kind in any product, service and/or company that could be construed as influencing the position presented in, or the review of, the manuscript entitled.

REFERENCES

- Faienza MF, Ventura A, Marzano F, Cavallo L. Postmenopausal osteoporosis: the role of immune system cells. *Clin Dev Immunol* 2013;2013:575936.
- Nicodemus KK, Folsom AR, Anderson KE. Menstrual history and risk of hip fractures in postmenopausal women. The Iowa Women's Health Study. *Am J Epidemiol* 2001;153:251-5.
- Lacko M, Schreierová D, Čellár R, Vaško G. The incidence of osteopenia and osteoporosis in patients with cementless total hip arthroplasty. *Acta Chir Orthop Traumatol Cech* 2015;82:61-6.
- Brown SR, Davies WA, DeHeer DH, Swanson AB. Long-term survival of McKee-Farrar total hip prostheses. *Clin Orthop Relat Res* 2002; 402:157-63.
- Iamthanaporn K, Chareancholvanich K, Pornrattanamaneewong C. Revision primary total hip replacement: causes and risk factors. *J Med Assoc Thai* 2015;98:93-9.
- Shao H, Shen J, Wang M, et al. Icarin protects against titanium particle-induced osteolysis and inflammatory response in a mouse calvarial model. *Biomaterials* 2015;60:92-9.
- Rahmy AIA, Gosens T, Blake GM, Tonino A, Fogelman I. Periprosthetic bone remodelling of two types of uncemented femoral implant with proximal hydroxyapatite coating: a 3-year follow-up study addressing the influence of prosthesis design and preoperative bone density on periprosthetic bone loss. *Osteoporos Int* 2004;15:281-9.
- Alm JJ, Mäkinen TJ, Lankinen P, Moritz N, Vahlberg T, Aro HT. Female patients with low systemic BMD are prone to bone loss in Gruen zone 7 after cementless total hip arthroplasty. *Acta Orthop* 2009;80:531-7.
- Lacko M, Schreierová D, Čellár R, Vaško G. Bone remodelling in the proximal femur after uncemented total hip arthroplasty in patients with osteoporosis. *Acta Chir Orthop Traumatol Cech* 2015;82:430-6.
- Finnilä S, Moritz N, Svedström E, Alm JJ, Aro HT. Increased migration of uncemented acetabular cups in female total hip arthroplasty patients with low systemic bone mineral density. A 2-year RSA and 8-year radiographic follow-up study of 34 patients. *Acta Orthop* 2016;87: 48-54.
- Aro HT, Alm JJ, Moritz N, Mäkinen TJ, Lankinen P. Low BMD affects initial stability and delays stem osseointegration in cementless total hip arthroplasty in women: a 2-year RSA study of 39 patients. *Acta Orthop* 2012;83:107-14.
- Qu S, Bai Y, Liu X, Fu R, Duan K, Weng J. Study on in vitro release and cell response to alendronate sodium-loaded ultrahigh molecular weight polyethylene loaded with alendronate sodium wear particles to treat the particles-induced osteolysis. *J Biomed Mater Res A* 2013;101: 394-403.
- Khatod M, Inacio MCS, Dell RM, Bini SA, Paxton EW, Namba RS. Association of bisphosphonate use and risk of revision after total hip arthroplasty: outcomes from a total joint replacement registry. *Clin Orthop Relat Res* 2015;473:3412-20.
- Warden SJ, Galley MR, Hurd AL, et al. Cortical and trabecular bone benefits of mechanical loading are maintained long term in mice independent of ovariectomy. *J Bone Miner Res* 2014;29:1131-40.
- Bouxsein ML, Boyd SK, Christiansen BA, Guldberg RE, Jepsen KJ, Müller R. Guidelines for assessment of bone microstructure in rodents using micro-computed tomography. *J Bone Miner Res* 2010;25:1468-86.
- Huang J, Zhou L, Wu H, et al. Triptolide inhibits osteoclast formation, bone resorption, RANKL-mediated NF- κ B activation and titanium particle-induced osteolysis in a mouse model. *Mol Cell Endocrinol* 2015;399:346-53.
- Knoch von F, Wedemeyer C, Heckelei A, et al. A comparison of the antiresorptive effects of bisphosphonates and statins on polyethylene particle-induced osteolysis. *Biomed Tech (Berl)* 2005;50:195-200.
- Iida-Klein A, Hughes C, Lu SS, et al. Effects of cyclic versus daily hPTH(1-34) regimens on bone strength in association with BMD, biochemical markers, and bone structure in mice. *J Bone Miner Res* 2005;21:274-82.
- Liu X, Zhu S, Cui J, et al. Strontium ranelate inhibits titanium-particle-induced osteolysis by restraining

- inflammatory osteoclastogenesis in vivo. *Acta Biomater* 2014;10:4912–8.
20. Knoch von M, Jewison DE, Sibonga JD, et al. Decrease in particle-induced osteolysis in obese (ob/ob) mice. *Biomaterials* 2004;25:4675–81.
 21. Sawyer A, Lott P, Titrud J, McDonald J. Quantification of tartrate resistant acid phosphatase distribution in mouse tibiae using image analysis. *Biotech Histochem* 2003;78:271–8.
 22. Dempster DW, Compston JE, Drezner MK, et al. Standardized nomenclature, symbols, and units for bone histomorphometry: a 2012 update of the report of the ASBMR Histomorphometry Nomenclature Committee. *J Bone Miner Res* 2013;28:2–17.
 23. Wong K-C, Cao S, Dong X, Law M-C, Chan T-H, Wong M-S. (-)Epiarznelechin protects against ovariectomy-induced bone loss in adult mice and modulate osteoblastic and osteoclastic functions in vitro. *Nutrients* 2017;9:530.
 24. Lin T-H, Tamaki Y, Pajarinen J, et al. Chronic inflammation in biomaterial-induced periprosthetic osteolysis: NF- κ B as a therapeutic target. *Acta Biomater* 2014;10:1–10.
 25. Sukur E, Akman YE, Ozturkmen Y, Kucukdurmaz F. Particle disease: a current review of the biological mechanisms in periprosthetic osteolysis after hip arthroplasty. *Open Orthop J* 2016;10:241–51.
 26. Pajarinen J, Kouri V-P, Jämsen E, Li T-F, Mandelin J, Kontinen YT. The response of macrophages to titanium particles is determined by macrophage polarization. *Acta Biomater* 2013;9:9229–40.
 27. Huang J-B, Ding Y, Huang D-S, et al. Inhibition of the PI3K/AKT pathway reduces tumor necrosis factor- α production in the cellular response to wear particles in vitro. *Artif Organs* 2013;37:298–307.
 28. Qin C-Q, Ding Y, Huang D-S, Xu J, Ma R-F, Huang J-B. Down-regulation of TNF- α by small interfering RNA inhibits particle-induced inflammation in vitro. *Artif Organs* 2011;35:706–14.
 29. Nich C, Marchadier A, Sedel L, Petite H, Vidal C, Hamadouche M. Decrease in particle-induced osteolysis in ovariectomized mice. *J Orthop Res* 2010;28:178–83.
 30. Nich C, Langlois J, Marchadier A, et al. Oestrogen deficiency modulates particle-induced osteolysis. *Arthritis Res Ther* 2011;13:R100.
 31. Nich C, Rao AJ, Valladares RD, et al. Role of direct estrogen receptor signaling in wear particle-induced osteolysis. *Biomaterials* 2013;34:641–50.
 32. Wang T, Liu Q, Zhou L, et al. Andrographolide inhibits ovariectomy-induced bone loss via the suppression of rankl signaling pathways. *Int J Mol Sci* 2015;16:27470–81.
 33. Akbar MA, Cao JJ, Lu Y, et al. Alpha-1 antitrypsin gene therapy ameliorates bone loss in ovariectomy-induced osteoporosis mouse model. *Hum Gene Ther* 2016;27:679–86.
 34. Viña J, Gambini J, García-García FJ, Rodríguez-Mañas L, Borrás C. Role of oestrogens on oxidative stress and inflammation in ageing. *Horm Mol Biol Clin Investig* 2013;16:65–72.
 35. Martín-Millán M, Castañeda S. Estrogens, osteoarthritis and inflammation. *Joint Bone Spine* 2013;80:368–73.
 36. Lerner UH. Inflammation-induced bone remodeling in periodontal disease and the influence of post-menopausal osteoporosis. *J Dent Res* 2006;85:596–607.
 37. D'Amelio P. The immune system and postmenopausal osteoporosis. *Immunol Invest* 2013;42:544–54.
 38. Honma M, Ikebuchi Y, Kariya Y, Suzuki H. Regulatory mechanisms of RANKL presentation to osteoclast precursors. *Curr Osteoporosis Rep* 2014;12:115–20.
 39. Chen S, Jin G, Huang K-M, et al. Lycorine suppresses RANKL-induced osteoclastogenesis in vitro and prevents ovariectomy-induced osteoporosis and titanium particle-induced osteolysis in vivo. *Sci Rep* 2015;5:12853.
 40. Kitaura H, Kimura K, Ishida M, Kohara H, Yoshimatsu M, Takano-Yamamoto T. Immunological reaction in TNF- α -mediated osteoclast formation and bone resorption in vitro and in vivo. *Clin Dev Immunol* 2013;2013:1–8.
 41. Sang C, Zhang Y, Chen F, et al. Tumor necrosis factor alpha suppresses osteogenic differentiation of MSCs by inhibiting semaphorin 3B via Wnt/ β -catenin signaling in estrogen-deficiency induced osteoporosis. *Bone* 2016;84:78–87.
 42. Adler RA, El-Hajj Fuleihan G, Bauer DC, et al. Managing osteoporosis in patients on long-term bisphosphonate treatment: report of a task force of the american society for bone and mineral research. *J Bone Miner Res* 2016;31:16–35.
 43. Gossiel F, Hoyle C, McCloskey EV, et al. The effect of bisphosphonate treatment on osteoclast precursor cells in postmenopausal osteoporosis: the TRIO study. *Bone* 2016;92:94–9.
 44. Knoch von M, Wedemeyer C, Pingsmann A, et al. The decrease of particle-induced osteolysis after a single dose of bisphosphonate. *Biomaterials* 2005;26:1803–8.
 45. Pan B, Farrugia AN, To LB, et al. The nitrogen-containing bisphosphonate, zoledronic acid, influences RANKL expression in human osteoblast-like cells by activating TNF- α converting enzyme (TACE). *J Bone Miner Res* 2004;19:147–54.
 46. Langdahl B, Ferrari S, Dempster DW. Bone modeling and remodeling: potential as therapeutic targets for the treatment of osteoporosis. *Ther Adv Musculoskelet Dis* 2016;8:225–35.
 47. Oteo-Álvaro Á, Matas JA, Alonso-Farto JC. Teriparatide (rh [1–34] PTH) improved osteointegration of a hemiarthroplasty with signs of aseptic loosening. *Orthopedics* 2011;34:e574–7.
 48. Zati A, Sarti D, Malaguti MC, Pratelli L. Teriparatide in the treatment of a loose hip prosthesis. *J Rheumatol* 2011;38:778–80.
 49. Hamano H, Takahata M, Ota M, et al. Teriparatide improves trabecular osteoporosis but simultaneously promotes ankylosis of the spine in the two mouse model for diffuse idiopathic skeletal hyperostosis. *Calcif Tissue Int* 2016;98:140–8.
 50. Moggetti B, Marino S, Barberis A, et al. Experimental stimulation of bone healing with teriparatide: histomorphometric and microhardness analysis in a mouse model of closed fracture. *Calcif Tissue Int* 2011;89:163–71.
 51. Kim JA, Ihn HJ, Park J-Y, et al. Inhibitory effects of trip-tolide on titanium particle-induced osteolysis and receptor activator of nuclear factor- κ B ligand-mediated osteoclast differentiation. *Int Orthop* 2015;39:173–82.
 52. Kiyama T, Okada S, Tanaka Y, et al. Inflammatory and necrotic effects of minodronate, a nitrogen-containing bisphosphonate, in mice. *Tohoku J Exp Med* 2013;230:141–9.
 53. Casanova M, Herelle J, Thomas M, et al. Effect of combined treatment with zoledronic acid and parathyroid hormone on mouse bone callus structure and composition. *Bone* 2016;92:70–8.
 54. Li W-L, Yu X, Huang Z-P, Pang Q-J. Effect of parathyroid hormone on healing in osteoporotic fractures via a phospholipase C-independent pathway. *J Int Med Res* 2017;45:1200–7.
 55. Vegger JB, Nielsen ES, Brüel A, Thomsen JS. Additive effect of PTH (1–34) and zoledronate in the prevention of disuse osteopenia in rats. *Bone* 2014;66:287–95.